JOURNAL OF THERMOPHYSICS AND HEAT TRANSFER
Vol. 9, No. 4, October–December 1995

Experiments in Acoustic Levitation: Surface Tension Measurements of Deformed Droplets

Yildiz Bayazitoglu* and Garrick F. Mitchell†
Rice University, Houston, Texas 77251

Acoustic levitation permits the observation of individual oscillating liquid droplets at low to moderate temperatures. Measurements of the oscillatory behavior of such droplets may be used to obtain thermophysical property measurements without the contaminating effects of a solid container. For example, for a droplet of spherical equilibrium shape, each mode of oscillation has been analytically shown to exhibit a single natural frequency that is a function of droplet size, mode number, and the surface tension and density of the liquid. In levitation experiments performed in Earth's gravity, however, this single frequency splits into multiple distinct frequencies, a phenomenon that may be attributed to the distorted equilibrium shape and the rotation of the droplet. In addition, the natural frequencies of droplets of highly volatile liquids change rapidly over time due to evaporation. This work presents experimental data and observations on the frequency splitting and surface tension of acoustically levitated samples of water and ethyl alcohol; the surface tension measured for both liquids came within 5% of the published value. In addition, a novel and relatively simple photodetection scheme for measuring oscillations as well as an improved method for modeling the ellipsoidal static shape deformation of the droplet are presented.

Nomenclature

$D(t)$ = droplet diameter at time t
D_0 = initial droplet diameter
K = rate of evaporation, m²/s
l, m = mode numbers
p_{ext} = externally applied pressure force
p_{lm}^r = radial projection of acoustic stress for mode l, m
R = equivalent spherical radius, cm
R_1, R_2 = local radii of curvature of droplet surface
$r(\theta, \phi, t)$ = shape of oscillating, deformed droplet
t = time
$X(\theta, \phi)$ = static deformation of droplet
$Y_{lm}(\theta, \phi)$ = spherical harmonic for mode l, m
Z = integral of product of three spherical harmonics
α = exponential coefficient of time dependence of ζ
$\beta(t)$ = frequency shift parameter
γ = surface tension, dyne/cm
γ_{exp} = mean experimental value of surface tension, dyne/cm
Δf_n = change in Rayleigh frequency for mode n
Δp = change in pressure across droplet surface
ζ_{lm} = coefficient of oscillatory deformation for mode l, m
$\zeta(\theta, \phi, t)$ = oscillatory deformation of droplet
θ = azimuthal angle in spherical coordinates
ρ = density, g/cm³
σ = surface of droplet
ϕ = polar angle in spherical coordinates
χ_{lm} = coefficient of static deformation for mode l, m
ω_l^* = inviscid (Rayleigh) frequency (rad/s unless noted)
ω_{lm} = natural frequency for mode l, m (rad/s unless noted)

Received Dec. 21, 1994; revision received April 7, 1995; accepted for publication April 10, 1995.

*Professor, Department of Mechanical Engineering and Materials Science, 6100 S. Main, P.O. Box 1892. Member AIAA.
†Graduate Student, Department of Mechanical Engineering and Materials Science, 6100 S. Main, P.O. Box 1892.

Introduction

THE determination of the thermophysical properties of substances is a time-consuming, but important, problem.[1] Such a property is surface tension, which plays an important role in, e.g., chemical processes where dispersed liquids interact with one another, and welding, where the behavior of a pool of molten metal determines the properties of the final weld. Surface tension is highly sensitive to contamination of the liquid sample (consider the effect of trace amounts of surfactants on the wetting properties of water); however, methods currently used to measure surface tension provide an avenue for such contamination, namely contact with a solid surface. Technological advancements, however, allow this contamination to be avoided through the "containerless" handling of materials, whether in the microgravity of Earth orbit or via ground-based levitation.

It has been known for some time[2–5] that surface tension determines the natural frequency of oscillation of a liquid droplet, as evidenced by the Rayleigh–Lamb equation[6,7]:

$$\omega_l^{*2} = \gamma l(l-1)(l+2)/\rho R^3 \tag{1}$$

The fundamental ($l = 2$) mode represents oblate–prolate oscillations, i.e., an alternating flattening and extension of the poles of the droplet. Some assumptions are employed in this equation:

1) The droplet viscosity is assumed negligible.
2) The medium in which the droplet levitates is of negligible density and viscosity.
3) The equilibrium shape of the droplet is a perfect sphere.
4) The amplitude of oscillations is small relative to the size of the droplet.
5) The restoring force arises solely from surface tension.
6) The droplet may not rotate so as to prevent centripetal and Coriolis forces.[8]

Subsequently, Miller and Scriven[2] analyzed the behavior of a viscous spherical droplet oscillating in a medium of ar-

bitrary viscosity. Such analyses have instigated efforts to determine the surface tension and viscosity of liquids from measurements of the natural frequency and damping rate of droplet oscillations. To accomplish such measurements, a droplet must somehow be levitated so that the contaminating effects of a container are removed. Levitation experiments have been performed in space, both on Skylab and on Space Shuttle missions (such as USML-1 onboard STS-50 from 25 June to 9 July 1992), where an external levitating force is required only to provide the driving force for oscillations and to position the droplet, correcting for fluctuations in microgravity. Here, liquid droplets assume the spherical shape with which the classical theory was derived as surface tension forces dominate over the body force of microgravity.

Earth-based levitation, meanwhile, offers a means by which the technique and apparatus involved in levitation may be refined much more easily and inexpensively before being applied in space. The presence of a gravitational field and the Earth's atmosphere, however, add several complicating factors to the classical hydrodynamic theory of oscillating drops in an inviscid medium. The viscosity of the "host" medium,[9] nonlinearity of oscillations,[10,11] and especially the aspherical equilibrium shape of levitated droplets[12,13] are some of the problems that have been examined in an effort to bring theory in line with experiment. While some investigators[2,3,9,10] have addressed the effect of viscosity on the oscillatory behavior of spherical liquid droplets, others[12–14] have focused on inviscid droplets whose equilibrium shape is aspherical due to the external force required to counteract gravity. Few analyses have addressed the effect of the static shape deformation on droplet oscillations. Cummings and Blackburn[13] analyzed the behavior of the fundamental ($l = 2$) mode of an aspherical droplet deformed by an electromagnetic levitating force and demonstrated a splitting of the frequency spectrum due to the deformation. Suryanarayana and Bayazitoglu[14] analyzed the effect of static deformation from an arbitrary external force and applied their findings to acoustic and electromagnetic forces, calculating the frequency splitting for modes $l = 2$, 3, and 4.

For the fundamental mode, the frequency spectrum splits into five separate frequencies for a droplet that rotates as it oscillates.[8,13,14] If the droplet does not rotate, this number decreases to three. The frequency splitting stems from the fact that, for modes $l \geq 2$, there exist $2l + 1$ different mode shapes m that reflect different behavior with respect to the polar angle ϕ (modes with $m = 0$ are axisymmetric). The five natural frequencies for the fundamental mode of a deformed rotating droplet, then, are $\omega_{2,-2}$, $\omega_{2,-1}$, $\omega_{2,0}$, $\omega_{2,1}$, and $\omega_{2,2}$. For a nonrotating droplet, it has been shown[13] that the dependence on the sign of m disappears, meaning that two of the five frequencies become degenerate. This leaves $\omega_{2,0}$, $\omega_{2,\pm1}$, and $\omega_{2,\pm2}$ as the three frequencies.

In the laboratory, researchers have several options for achieving levitation in Earth's gravity. These are summarized by Barmatz,[15] who describes such techniques as aircraft flights of parabolic trajectory, drop tubes, and stationary levitation by acoustic, electromagnetic, aerodynamic, and electrostatic means. This work considers acoustic levitation, in which a modulated acoustic pressure wave provides both the levitating force and the driving force for oscillations (see the Experimental Apparatus section). Terrestrial acoustic levitation experiments initially involved the levitation of droplets in an immiscible liquid, as described in Marston and Apfel[16] and Trinh et al.[17] In liquid–liquid systems, the similarity in density between the droplet and the host medium allows large (>1-cm-diam) droplets to be levitated with minimal levitating force. However, the viscosity of the outer medium is clearly not negligible in this case. Recently, investigations of liquid droplets levitated in air were performed by Trinh and Hsu[18] and Tian et al.[19] with respect to the equilibrium shape of levitated droplets, by Trinh and Hsu[20] and Trinh, Marston, and Robey[21] with respect to the measurement of density and surface tension, and by Daidzic et al.[22] with respect to droplet evaporation.

No analyses have been presented that combine the effects of viscosity and aspherical equilibrium shape on the oscillatory behavior of liquid droplets. As will be shown, the levitation method described here has difficulty dealing with highly viscous liquids such as heavy oils, so the approach used here begins from the inviscid limiting case. This work uses substantially deformed (ellipsoidal) droplets of relatively low viscosity liquids such as water and ethyl alcohol in an effort to combine the viscous and aspherical conditions. The experiment described herein is applicable to liquids of surface tension $\gamma > 20$ dyne/cm, viscosity $\nu \leq 2$ cSt, density $\rho < 10$ g/cm^3, and droplets between 1–4 mm in diameter.

Experimental Apparatus

The apparatus used in this experiment is relatively compact and fits on a desktop; a diagram of the setup is shown in Fig. 1. The theory and use of the acoustic levitator is well documented in the literature.[16,17,20,21] A high-intensity acoustic wave is generated by an ultrasonic piezoelectric transducer driven at its resonant frequency of 20 kHz. A vertical aluminum horn is attached axially to the transducer. The ultrasonic wave radiates from the tip of the horn and is reflected by a concave reflector whose distance from the horn is adjusted via a micrometer head. When the horn and the reflector are separated by an appropriate distance, a standing wave is set up in the gap. The acoustic pressure varies as the square of a sine wave along the horn-reflector axis,[20] forming periodic planes of locally minimized pressure. The concavity of the acoustic reflector serves to radially focus these planes of low pressure into points at which a droplet of liquid (or even a small solid object) may be stably levitated against gravity. In this experiment, a separation of one and one-quarter wavelength is used, and two pressure nodes are created as a result (this is shown in Fig. 2, where two droplets may be seen to levitate simultaneously in the levitator). In order to induce droplet oscillations, the 20-kHz carrier wave is sinusoidally modulated at the desired frequency of oscillation. In this experiment, droplet natural frequencies ranged between about 40–200 Hz. The acoustic levitator causes oblate–prolate oscillations that correspond to the fundamental ($l = 2$) mode of the droplet. A resistive load in parallel with the transducer dissipates the energy of the horn; otherwise, the horn's inertia would prevent small modulations of the drive signal from being realized in the amplitude of the acoustic wave.

Aside from the levitator itself, the most crucial part of the experimental apparatus is that which measures droplet oscillations. A primary advantage of the single-axis acoustic lev-

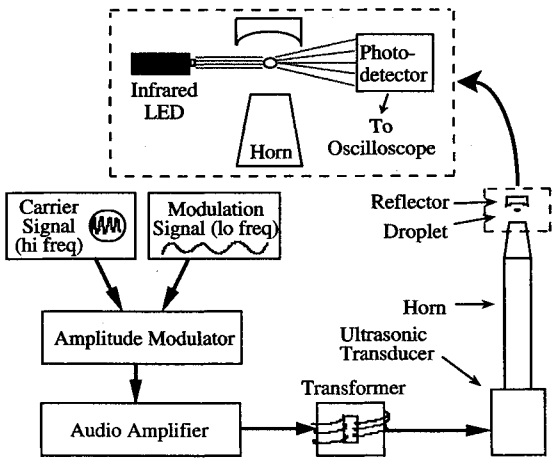

Fig. 1 Schematic diagram of levitator and photodetector.

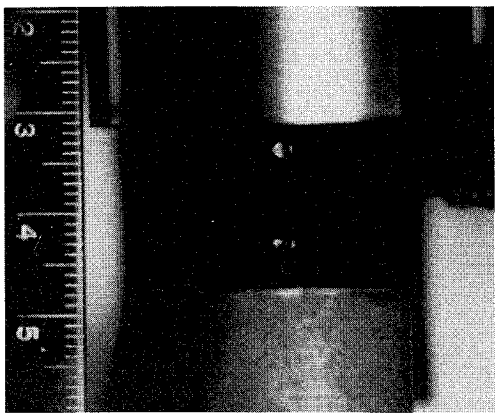

Fig. 2 Photograph of levitated water droplets.

itator is that the object being levitated is visible in all directions perpendicular to the levitator axis. As such, some investigators have used high-speed cameras, analyzing the film frame-by-frame to determine mode shapes and frequencies of oscillation.[23] Subsequent approaches to droplet oscillation measurement involve photometry, such as Marston's and Apfel's rainbow interferometry,[16] extinction methods,[20] and digital image processing.[1] The mode shapes themselves must also be identified, but oscillations of an amplitude large enough to be seen directly introduce additional nonlinearities to the system as described by Daidzic.[11] This makes the direct identification of mode shapes quite difficult, especially with respect to axisymmetry. This was attempted by backlighting the droplet with a bank of light emitting diodes (LEDs) driven by a pulse generator at twice the modulation frequency. The limited results obtained in this way were corroborated by theoretical predictions,[13,14] and since all droplets considered here experienced similar forces and static deformations, the location of the axisymmetric mode with respect to the others was taken to be constant.

This experiment uses a simple and compact device to measure the relative amplitude of droplet oscillations. An infrared (IR) LED and matching photodetector are placed on opposite sides of the levitating droplet as shown in Fig. 1. This alternating current (AC) coupled device outputs a voltage signal proportional to the rate of change of light transmitted through the droplet. The changes in the intensity of light reaching the photodetector are directly related to changes in the shape of the droplet; hence, the shape oscillations appear as a sine wave in the output from the photodetector. When the amplitude of the sine wave reaches a maximum with respect to frequency, the instantaneous frequency of the modulation signal corresponds to a natural frequency of the droplet. The photodetector signal is filtered to remove the unwanted effects of the droplet wandering about the potential well and then amplified and displayed on an oscilloscope that is triggered from the modulation signal. The advantages of this photodetection technique mainly lie in its simplicity. Since the mode number is assumed known and droplet size measurement may be made with a video or still camera, all that must be determined is the point at which the oscillations are the most vigorous. No lasers are required, power requirements are minimal, and the photodetector's influence on the droplet itself is basically nil.

Analysis

This work seeks to experimentally prove the results of Suryanarayana and Bayazitoglu[14] in which the effect of static deformation due to an arbitrary external levitating force, especially as regards the splitting of the frequency spectrum into either three or five separate peaks, is studied. Their work treats the shape of the droplet as a sphere of radius R distorted by a static deformation $X(\theta, \phi)$ and a time-dependent (oscillatory) deformation $\zeta(\theta, \phi, t)$, both of which are small compared to the size of the droplet:

$$r = R + X(\theta, \phi) + \zeta(\theta, \phi, t) \tag{2}$$

The deformation components X and ζ are assumed to be small relative to the droplet diameter and are expandable in spherical harmonics:

$$X(\theta, \phi) = \sum_{uv} \chi_{uv} Y_{uv}(\theta, \phi) \tag{3a}$$

$$\zeta(\theta, \phi, t) = \sum_{lm} \zeta_{0lm} e^{-\beta t} Y_{lm}(\theta, \phi) \tag{3b}$$

The static deformation is assumed to be axisymmetric; this condition was experimentally observed by Tian et al.[19] The surface of the droplet is defined by the equation:

$$\sigma = r - [R + X(\theta, \varphi) + \zeta(\theta, \varphi, t)] = 0 \tag{4}$$

In an Earth-based liquid levitation experiment in air, the static deformation of the droplet to some degree is unavoidable as the body force of gravity is balanced by the acoustic levitating force. Meanwhile, surface tension forces increase as droplet size decreases (due to the $1/R$ functional dependence), meaning that only very small (<1 mm) droplets begin to approximate spheres. However, since the amplitude of oscillations is required to be small compared to the droplet diameter for the sake of linear behavior, the oscillations to be observed would be vanishingly small and difficult to detect, even with the photodetection technique to be described later. To counter this, some investigators[13,14] have performed analyses of aspherical, inviscid levitated droplets. The stipulation of asphericity, however, requires a relatively small static deviation from the sphere in addition to small amplitude oscillations. For large (>2-mm-diam) water droplets, and smaller droplets of liquids with low surface tension, the static droplet shape can have an AR (i.e., ratio of width to height) in excess of 2.0.

The analysis performed in Ref. 14 treats the acoustic surface force acting on the droplet to first-order and assumes that the quadrupole term of the radial projection of the acoustic stress p'_{20} dominates so that the radial projection of the acoustic pressure force acting on the droplet is completely represented by $p'_{20}Y_{20}$. Such a force is only capable of inducing the mode-2 (prolate–oblate) oscillations observed in experiments. As a result, the static distortion X of the droplet is assumed to take the shape of the second-order spherical harmonic Y_{20}. It has been found in the course of this work, however, that beyond an AR of about 1.3, the previous assumption no longer faithfully reflects the shape of the droplet. Adding the second harmonic to a sphere in order to obtain the measured height and width of a highly deformed droplet yields an oblate shape that "pinches in" on itself at the poles, while the droplet itself can be observed to maintain an ellipsoidal shape. If, however, the static shape deformation X is expanded to include a fourth-order term

$$X(\theta, \phi) = \chi_{20} Y_{20}(\theta, \phi) + \chi_{40} Y_{40}(\theta, \phi) \tag{5}$$

the assumed droplet shape much more closely matches the observed shape (see Fig. 3). The deformation coefficients χ_{20} and χ_{40} may be found by an iterative technique that minimizes the least-squares difference between the harmonic approximation and an ellipsoid having major and minor axes of the same dimensions as the droplet in question. This suggests that, at least for droplets whose static deformation exceeds some value, higher-order acoustic pressure effects must be considered.

To summarize the analysis being considered here,[14] the boundary conditions applied to the surface $\sigma = 0$ in the equa-

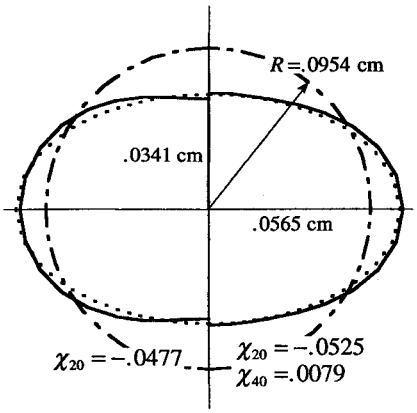

Fig. 3 Comparison of static shape modeling methods.

tions of motion are the kinematic condition, which equates the radial velocity of the droplet to the time rate of change of the droplet shape $\partial\zeta/\partial t$, and a normal force balance relating the pressure change across the boundary to the surface tension γ and the external force p_{ext}:

$$\Delta p = \gamma(1/R_1 + 1/R_2) + p_{\text{ext}} \tag{6}$$

where p_{ext} is expanded in spherical harmonics and deformation coefficients $p_{l,m}$:

$$p_{\text{ext}} = \sum p_{l,m}^{n} \left(\frac{R + X + \zeta}{R}\right)^{n} Y_{l,m}(\theta, \phi) \tag{7}$$

and Δp is found from the expression for radial velocity. The normal force balance is used to obtain the "complete surface condition" for the droplet [Eq. (27) in Ref. 14]. Comparing like terms, the time-independent terms of the equation relate the external force to the static surface energy of the droplet (which, judging by the nonspherical droplet shape, is increased over the spherical droplet), and the mode-1 terms balance the force of gravity and determine the equilibrium position of the droplet for density analyses.[19,20] The higher mode terms relate higher mode components of the external force to the corresponding components of the droplet deformation.

Ignoring translational frequencies and assuming that the external force is the same as if the droplet were spherical, Eq. (35) in Ref. 14 gives the first-order ($n = 0$) solution for a droplet oscillating in mode l under the influence of an externally applied force as

$$\omega_{l,m}^2 = \omega_l^{*2} + \frac{1}{\rho R^2} p_{u,0} \left[\frac{3l(l-1)(l+2)}{(u-1)(u+2)} + \frac{2lu(u+1)}{(u-1)(u+2)}\right] Z_{2,u,2}^{m,0,m} \tag{8}$$

where the second subscript of p is zero to reflect the axisymmetry of the external force. The symbol Z is a shorthand representation for the integral of the product of three spherical harmonics. Such products appear frequently in the literature[14]:

$$Z_{l'',l',l}^{m'',m',m} = \int_{-1}^{1} \int_{0}^{2\pi} Y_{l''}^{m''*}(u, \phi) Y_{l'}^{m'}(u, \phi) Y_{l}^{m}(u, \phi)\, d\phi\, du \tag{9}$$

The only nonzero values of the integral in Eq. (8) are $Z_{2,2,2}^{m,0,m}$ and $Z_{2,4,2}^{m,0,m}$. For mode-2 oscillations, taking into account both second- and fourth-order components of the static shape deformation, Eq. (8) becomes

$$\omega_{2,m}^2 = \omega_2^{*2} + (1/\rho R^2)[p_{2,0}(12)Z_{2,2,2}^{m,0,m} + p_{4,0}(52/9)Z_{2,4,2}^{m,0,m}] \tag{10}$$

Equation (10) is identical to Eq. (53) in Ref. 14, which applies to electromagnetic levitation and includes the fourth-order spherical harmonic in the magnetic pressure distribution.

In the first-order approximation, the static shape deformation coefficients χ are related to the p by the expression:

$$\chi_{uv} = -\frac{R^2}{\gamma}\left[\frac{1}{(u-1)(u+2)}\right] p_{uv} \tag{11}$$

Since the experimental approach allows the direct measurement of the static shape deformation, Eq. (11) is solved for p_{uv} in terms of χ_{uv} and substituted into Eq. (10):

$$\omega_{2,m}^2 = \omega_2^{*2} + (-\gamma/\rho R^4)(48\chi_{2,0}Z_{2,2,2}^{m,0,m} + 104\chi_{4,0}Z_{2,4,2}^{m,0,m}) \tag{12}$$

Here, the values of the triple integrals are independent of the sign of m, just as the mode shapes for a nonrotating droplet. Substituting these values, which are tabulated in Ref. 14, yields expressions for the three frequencies of oscillation as functions of the measured static shape deformation coefficients:

$$\omega_{2,0}^2 = \omega_2^{*2} - (\gamma/\rho R^4)(8.6507\chi_{20} + 25.1467\chi_{40}) \tag{13a}$$

$$\omega_{2,\pm 1}^2 = \omega_2^{*2} - (\gamma/\rho R^4)(4.3254\chi_{20} - 16.7645\chi_{40}) \tag{13b}$$

$$\omega_{2,\pm 2}^2 = \omega_2^{*2} - (\gamma/\rho R^4)(-8.6507\chi_{20} + 4.1911\chi_{40}) \tag{13c}$$

Neglecting the χ_{40} terms, the previous equations are identical to Eqs. (40) in Ref. 14. In an acoustic levitator, droplets take on an oblate equilibrium shape, and χ_{20} is negative. Hence, the analysis predicts that $\omega_{2,0} > \omega_{2,\pm 1} > \omega_{2,\pm 2}$, and $\omega_{2,0}$ and $\omega_{2,\pm 1}$ lie above the Rayleigh frequency, while $\omega_{2,\pm 2}$ lies below. If the χ_{40} terms are included, the trends may change depending on the sign and magnitude of χ_{40} itself. As will be shown, however, χ_{40} is positive and an order of magnitude smaller than χ_{20}, and so the order of the three frequencies remains the same, although $\omega_{2,0}$ and $\omega_{2,\pm 1}$ come even closer together. Note that the earlier expressions obey the relation between the split frequencies and the Rayleigh frequency offered by Cummings and Blackburn[13]:

$$\left[\frac{1}{(2l+1)}\right] \sum_{m=-l}^{l} \omega_{lm}^2 = \omega_l^{*2} \tag{14}$$

This expression may be viewed as equating the spectral energies of the split spectrum and the inviscid frequency, which is $2l + 1$ degenerate.

The results of this correction to the analysis of levitated droplets will be of considerable importance in refining levitation experiments performed in Earth's gravity, because liquids with low surface tension, such as ethyl alcohol and low-viscosity silicone oils, are deformed much more than, e.g., water due to the decreased surface tension forces present. With the results of this experiment, a far wider range of liquids may be feasibly tested using acoustic levitation.

Results and Discussion

The majority of data collected in this experiment use water as the levitated liquid. The high surface tension of water enables larger droplets to be stably levitated, whereas its relatively low viscosity is useful because this experiment has so far neglected viscous effects. In addition, the published properties of water serve as a check for the results presented here.

Results for ethyl alcohol and tap water, which contains various impurities, and hence, should have a lower surface tension than distilled water, are also shown.

Of particular interest is the fact that only two distinct resonant peaks could be found for levitated droplets in this experiment. As the modulation frequency is being swept, three separate "events" are seen by the photodetector, and they are spaced roughly equally as in the first spectrum plotted by Trinh et al.[21] Upon closer inspection, however, the frequency of this peak remains constant over time, in sharp contrast to the other peaks that shift slowly but steadily upward in frequency as the droplet evaporates. In addition, the frequency of this lowest peak lies far below the values predicted by theory. This seems to indicate an optical signature of something different than oblate–prolate oscillations. Since this lowest peak remains fixed in the frequency domain, it is believed to represent a translation of the droplet that could be an artifact of the signal used to drive the transducer. Translational frequencies may be ignored because they correspond to the $l = 1$ mode and exist separately from the $l = 2$ fundamental mode oscillations.

For droplets where three resonant peaks besides the "false" peak were found, the two higher peaks were very close together (within 5 Hz). This seems to suggest that, in cases where only two peaks are found, the higher of these two peaks is actually two separate frequencies that cannot be individually distinguished by this apparatus. Indeed, in the acoustic case the frequency splitting predicted by Suryanarayana and Bayazitoglu[14] is asymmetric, with two of the frequencies lying above the Rayleigh frequency and much closer together than they are to the third frequency. Cummings and Blackburn[13] make similar predictions; Fig. 3 of their paper, on which Fig. 4 is based, shows the expected effects of χ_{20} and χ_{40} on the frequency split. Here, a negative χ_{20} can be seen to shift $\omega_{2,0}$ and $\omega_{2,\pm1}$ upward and $\omega_{2,\pm2}$ downward, whereas a positive χ_{40} shifts $\omega_{2,0}$ downward, $\omega_{2,\pm1}$ upward, and affects $\omega_{2,\pm2}$ only slightly. Superimposing these two effects while scaling down the χ_{40} effect (since $\chi_{40} < \chi_{20}$ for the droplets in this experiment) brings $\omega_{2,0}$ and $\omega_{2,\pm1}$ even closer together as shown in Fig. 4. It seems feasible, then, to say that the higher resonant peak is approximately the average of the $\omega_{2,0}$ and $\omega_{2,\pm1}$ frequencies. This assumption generates most of the uncertainty in the results[24]; however, in the absence of greater frequency resolution it must be made. Viscous effects contribute to the lack of resolution by "rounding off" the resonant peaks and obscuring fine details in the frequency spectrum. Along the same lines, high-viscosity fluids, such as heavy oil, are unsuitable for use with this apparatus because the peaks in their frequency spectra are so broad as to be indistinguishable from background noise.

The input data in this experiment are the measured natural frequencies in Hz and the width and height of the droplet as measured along the axes of symmetry of a photograph of the droplet viewed from the side. The radius of a spherical droplet having the same volume as the deformed droplet is found by assuming the droplet to be an ellipsoidal body of revolution with semimajor and semiminor axes as measured. This equivalent spherical radius is used in the Rayleigh–Lamb equation along with the anticipated surface tension (for liquids whose values are already known) to compute the inviscid frequency for the droplet. The values of the static deformation coefficients χ_{20} and χ_{40} are then found using an iterative technique that minimizes the least-squares error between the radii of the ellipsoidal droplet and the analytically assumed shape

$$r(\theta, \phi) = R + (\chi_{20}Y_{20} + \chi_{40}Y_{40}) \tag{15}$$

This, along with the density of the liquid, is sufficient to apply Eqs. (13) and make an analytical prediction for the frequency splitting.

Data for distilled water and ethyl alcohol at 24°C are shown in Table 1 and Table 2, respectively. Surface tension measurements by other means were not available at the time these data were collected; hence, for droplets of liquids whose properties are well established, the radius of a sphere having the same volume as the droplet was calculated and used in the Rayleigh–Lamb equation along with the published values of surface tension and density to yield the inviscid frequency ω_2^* in rad/s. Based on the inviscid frequency and the calculated static shape deformation coefficients χ, Eqs. (13) are then used to predict $\omega_{2,0}$, $\omega_{2,\pm1}$, and $\omega_{2,\pm2}$. An experimental value of surface tension γ_{exp} is evaluated using Eqs. (14) and (1), with the higher of the two natural frequencies being treated as the average of $\omega_{2,0}$ and $\omega_{2,\pm1}$. The mean value of γ_{exp}, 75.8 dyne/cm, is 5% above the published value of 72.2 dyne/cm; the uncertainty based on 20:1 odds is ±7.3 dyne/cm, due to the difficulty in separating the $\omega_{2,0}$ and $\omega_{2,\pm1}$ frequencies. The measured, predicted, and inviscid frequencies for distilled water are plotted against the droplet radius in Fig. 5.

As a side note, data for tap water and commercially bottled "distilled water" were also collected. The measured frequencies are averaged as in Eq. (14) to yield the inviscid frequency and permit the calculation of γ_{exp}. The mean value of γ_{exp} is taken to be the surface tension of the unknown. The Rayleigh frequencies and frequencies from Eqs. (13) are then based on γ_{exp}. As shown in Table 3, the surface tension value for tap water is 14.1% lower than that of distilled water, which is as expected due to the impurities present. The store-bought distilled water, meanwhile, has a surface tension that is higher than that of the tap water, but still below the published value by 13%, indicating this water would be unsuitable for sensitive laboratory use.

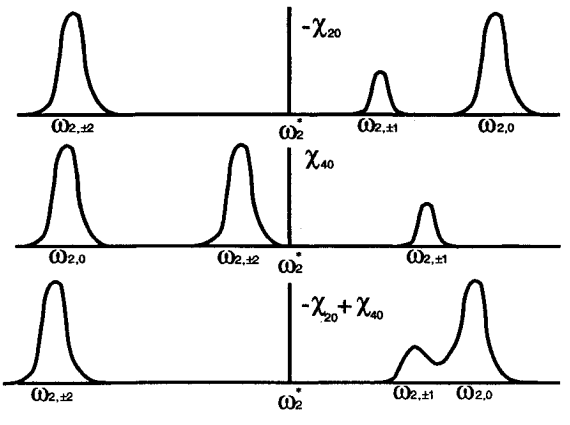

Fig. 4 Expected frequency splitting for various static shape deformations.

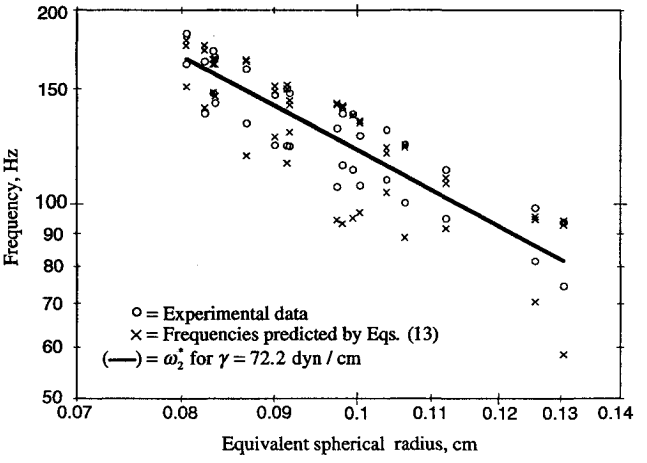

Fig. 5 Frequency data for distilled water.

Table 1 Experimental data for distilled water

R_{sphere}, cm	χ_{20}	χ_{40}	Observed frequencies, Hz $\omega_{2,\pm2}$	Observed frequencies, Hz $\omega_{2\pm1}$	Observed frequencies, Hz $\omega_{2,0}$	ω_2^{*},[a] Hz	γ_{exptl},[b] dyne/cm	Predicted frequencies, Hz[c] $\omega_{2,\pm2}$	Predicted frequencies, Hz[c] $\omega_{2,\pm1}$	Predicted frequencies, Hz[c] $\omega_{2,0}$
0.0833	−0.0095	0.0003	148.6	173.0		163.68	76.20	148.99	164.84	167.86
0.1064	−0.0334	0.0031	100.4	123.65		114.92	78.28	88.65	122.44	123.28
0.1257	−0.0367	0.0032	81.55	98.6		92.16	83.01	70.41	94.57	95.57
0.0835	−0.0107	0.0004	143.5	169.15		159.39	72.78	147.12	164.99	168.16
0.0901	−0.0159	0.0009	123.5	147.85		138.62	69.17	127.04	149.60	152.51
0.0918	−0.0099	0.0004	123.0	148.7		138.99	73.55	129.25	142.29	144.63
0.0824	−0.0178	0.0012	138.4	166.8		156.06	67.05	141.07	173.43	176.53
0.0805	−0.0129	0.0007	165.1	184.0		176.68	80.14	152.11	176.19	179.63
0.1122	−0.0195	0.001	94.95	113.0		106.15	78.32	91.56	107.54	109.73
0.0915	−0.0245	0.0019	109.45	123.25	151.1	140.62	74.55	115.72	150.90	153.10
0.0982	−0.0379	0.0042	114.9	138.2		129.38	78.01	93.15	141.86	140.95
0.0975	−0.0374	0.0041	106.4	131.15		121.85	67.73	94.37	143.26	142.45
0.1039	−0.016	0.0007	109.2	130.3		122.30	82.55	104.18	119.86	122.32
0.1303	−0.0552	0.0066	74.55	93.65		86.52	81.49	58.44	94.12	92.81
0.0869	−0.0283	0.0027	133.55	162.25		151.42	74.05	118.79	166.61	167.47
0.1004	−0.0313	0.0029	106.9	127.7		119.81	71.49	96.90	133.44	134.51
0.0995	−0.0346	0.0035	113.05	137.8		128.47	80.01	94.95	137.10	137.30

[a]Rayleigh frequency computed using Eq. (14).
[b]Applying calculated Rayleigh frequency and equivalent spherical radius in Eq. (1).
[c]From Eqs. (13).

Table 2 Experimental data for ethyl alcohol

R_{sphere}, cm	χ_{20}	χ_{40}	Observed frequencies, Hz $\omega_{2,\pm2}$	Observed frequencies, Hz ω_{2+1}	Observed frequencies, Hz $\omega_{2,0}$	ω_2^{*},[a] Hz	γ_{exptl},[b] dyne/cm	Predicted frequencies, Hz[c] $\omega_{2,\pm2}$	Predicted frequencies, Hz[c] $\omega_{2,\pm1}$	Predicted frequencies, Hz[c] $\omega_{2,0}$
Without correction for evaporation										
0.0688	−0.026	0.0028		119.30		119.30	17.95	100.59	151.42	150.75
0.0867	−0.0429	0.0059	74.90		93.80	86.74	19.05	61.70	111.69	108.10
0.0954	−0.0525	0.0079	69.50		78.60	75.09	19.02	49.05	98.84	94.21
0.0945	−0.0414	0.0051	69.10		80.40	76.08	18.94	58.39	96.16	61.13
0.0933	−0.0354	0.0039	71.40		81.60	77.68	18.99	63.56	95.96	95.46
0.069	−0.0204	0.0018	117.4		131.9	126.30	20.33	108.24	146.14	147.56
0.0976	−0.0412	0.0049	64		78.9	73.30	19.37	56.70	91.06	89.79
0.0949	−0.0446	0.0058	67		78.8	74.31	18.28	55.76	96.75	94.32
0.0883	−0.0286	0.0027	79.6		91.8	87.13	20.24	72.97	102.08	102.65
0.0949	−0.0376	0.0043	71.2		80.6	76.98	19.63	60.90	94.06	93.31
0.079	−0.0232	0.002	94.7		107.6	102.63	20.12	88.59	119.27	120.54
Using frequency averaging to account for evaporation										
0.0973	−0.0341	0.0035	61.3		76.8	71.01	18.03	61.46	89.02	89.07
0.1147	−0.0606	0.0088	48		59.2	54.99	17.69	38.59	74.43	71.36
0.0717	−0.0011	0		124.8		116.32	22.30	124.00	125.66	126.13
0.0732	−0.0252	0.0025		133.65		133.65	27.14	94.83	136.22	136.48
0.0624	−0.0149	0.0011	123.9		180.8	160.48	24.27	132.05	166.43	169.09

[a]Rayleigh frequency computed using Eq. (14).
[b]Applying calculated Rayleigh frequency and equivalent spherical radius in Eq. (1).
[c]From Eqs. (13).

Highly volatile liquids provide their own challenges in measuring surface tension via levitation. As described by Daidzic[22] and other experimenters,[18] a consequence of evaporation is a continuous upward shift of the natural frequencies of a droplet over time due to the decrease in mass, which is proportional to the decrease in the size of the droplet:

$$D(t)^2 = D_0^2 - Kt \tag{16}$$

where $D(t)$ is the droplet diameter at time t, D_0 is the diameter at time $t = 0$, and K is the rate of evaporation of the liquid. For a highly volatile liquid such as ethyl alcohol, the rate of evaporation, and hence, the frequency shift, can be such that the time required to measure the natural frequencies and photograph the droplet is a significant parameter. The change in the Rayleigh frequency Δf_n is shown[22] to be a function of

Table 3 Comparison of experimentally measured and published surface tension values (dyne/cm)

Liquid	γ_{mean}[a]	$\gamma_{published}$[b]	% Error
Distilled water	75.8 ± 7.3	72.2	5.0
Tap water	62.0 ± 7.0	——	——
Bottled water	62.8 ± 6.9	——	——
Ethyl alcohol[c]	19.3 ± 4.1	22.4	−13.8
Ethyl alcohol[d]	20.8 ± 4.2	22.4	−7.1
Ethyl alcohol[e]	21.9 ± 4.2	22.4	−2.3

[a]Uncertainty based on 20:1 odds.
[b]At 24°C; interpolated from data in *Handbook of Chemistry and Physics*, 69th ed., CRC Press, Boca Raton, FL, 1988.
[c]Evaporation not taken into account.
[d]Frequencies incremented to account for evaporation between frequency and size measurements.
[e]Droplet size averaged to time at which frequencies were measured.

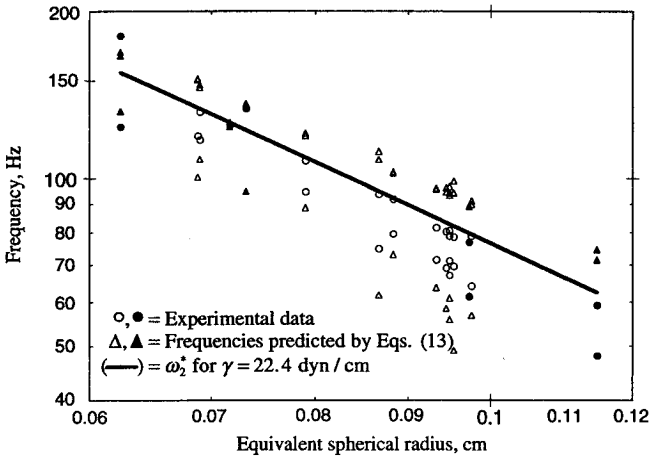

Fig. 6 Frequency data for ethyl alcohol. Drops for which evaporation was taken into account are denoted by the filled symbols.

the natural frequency at some reference time $f_n^{D_0}$ and a time parameter $\beta(t)$, which itself is a function of the rate of evaporation K and the elapsed time:

$$\Delta f_n = \beta(t) \times f_n^{D_0} \tag{17}$$

From Daidzic,[22] for a 2 mm diam drop of ethyl alcohol, $\beta(t = 30\text{ s}) = 0.0392$, meaning that an error of 3.92% in the frequency readings is predicted if the droplet size is measured only after 30 s are spent in measuring the frequency spectrum (a reasonable length of time). This error is exacerbated by the fact that the rate of evaporation, and hence, the rate of the frequency shift, is increased as a result of the standing wave, with the effect being directly proportional to the pressure.[22] As a result, the larger the droplet, the higher the acoustic pressure required for levitation, and the faster the frequencies increase over time.

The hollow circles in Fig. 6 show frequency data for ethyl alcohol where the size of the droplet was measured after the natural frequencies were found. As expected, the measured surface tension of 19.3 dyne/cm is lower than the published value of 22.4 dyne/cm, because the size of the droplet when photographed was considerably smaller than the size for which the frequency spectrum was measured. To compensate for evaporation, which increases the natural frequencies over time, the frequencies were incremented by 3.92% as described earlier. The revised value of γ_{exp}, 20.8 dyne/cm, is much closer to the published value as shown in Table 3, but is still 7.1% lower. The remaining difference would seem to be due to the enhanced evaporation from the acoustic standing wave described in Ref. 22. Since the intensity of the standing wave was tailored to each droplet, however, an attempt to quantify this effect is not made here. Another means of circumventing the frequency shift is simply to measure the natural frequencies both before and after the size of the droplet is measured and take their average values. This method yielded γ_{exp} = 21.9 dyne/cm, only 2.3% below the published value. Short droplet life and the instability of ethyl alcohol droplets, however, required several experimental trials to successfully collect the data for a single droplet. The results are shown in Table 3 and by the filled symbols in Fig. 6. The uncertainty of the data is high (±4 dyne/cm) due to the combination of two of the frequencies described earlier.

Uncertainty Analysis

In calculating the surface tension of a liquid using Eq. (1), uncertainties are introduced through the measurements of droplet size and the natural frequencies. In addition, small variations in the air temperature create uncertainty in the density of the liquid sample, which in turn affects other calculated quantities. Here, uncertainties are reported using 20:1 odds; a more complete account of the analysis may be found in Ref. 24. While the precision of the frequency counter allowed a resolution of 0.01 Hz, the reading wandered sufficiently to generate an uncertainty of ±0.1 Hz. An uncertainty of ±1 Hz was assigned to each value of $\omega_{2,\pm1}$ due to the difficulty in distinguishing it from the $\omega_{2,0}$ frequency. Indeed, this aspect of the experiment was the source of most of the uncertainty in the results, especially in light of the fact that the $\omega_{2,\pm1}$ frequency is counted twice in the weighted average of Eq. (14). Repeated size measurements of various drops showed the uncertainty of the measured size of a droplet to be $\pm 85 \times 10^{-4}$ cm; still photographs proved much more precise than the use of a video camera for the purposes of size measurements. While the apparatus was not placed in a strictly temperature-controlled environment, room temperature was always 24 ± 0.5°C. Within this range, the variation in the liquid density ρ was taken as ±0.005 g/cm³. In addition, the mode number l is taken to be exact.

It is clear that the procedure for testing volatile liquids could have easily used a single set of natural frequency measurements preceded and followed by droplet size measurements that could then be averaged. However, the opposite approach was chosen because measuring the frequencies twice and then taking their averages, while being experimentally difficult, helped offset the small sample bias of an already uncertain measurement.

Conclusions

Experimental observations and numerical data concerning the natural frequencies of acoustically levitated oscillating droplets are presented. The focus in this study has been on ellipsoidal liquid droplets of relatively low, albeit finite, viscosity. Results from an analysis of aspherical, inviscid droplets[14] have been used to reduce these data, and although the conditions of zero viscosity and small deviation from a spherical equilibrium shape were violated, the results show good agreement with published results for distilled water and ethyl alcohol. The uncertainty of these results is on the order of ±10% for water and ±20% for ethyl alcohol due to the closeness of the $\omega_{2,\pm1}$ and $\omega_{2,0}$ frequencies. Viscous effects make the $\omega_{2,\pm1}$ resonance almost impossible to locate by "blurring" the frequency spectrum; greater frequency resolution is needed to overcome this phenomenon. With the use of a refined static shape deformation model, however, the analysis in Ref. 14 predicts the proximity of two of the natural frequencies for acoustically levitated droplets. These results are encouraging in evaluating analytical predictions for frequency splitting.[14] It has also been shown that, with a simple apparatus and rapid approach to data collection, even highly volatile liquids may be tested using levitation.

Comparisons between experimental data and analytical predictions concerning the natural frequencies of deformed levitating droplets are instructive for evaluating the state of knowledge of the forces acting on an acoustically levitated droplet. If the influence of the modulated acoustic standing wave on the droplet can be known, then its impact on observed thermophysical properties may be evaluated as well. For the time being, however, fairly accurate results have been realized from a simple, inexpensive, and compact apparatus.

Naturally, the question arises as to why the droplet should not follow the shape of the second-order spherical harmonic Y_{20} as the level of distortion increases. One possible explanation involves the radial focus of the pressure node that is required to hold the droplet in position from side-to-side. This focus is achieved through the use of a slightly concave acoustic reflector. For the apparatus used in this experiment, various reflectors were fabricated to determine which radius of curvature provided sufficient radial focus to hold the droplet stationary. For the sake of simplicity, the curvature of the reflectors was spherical. A reflector with a gentle radius of curvature (on the order of 5 in.) required an exceptionally

high standing wave intensity to hold the droplet with an acceptable amount of side-to-side "wandering," whereas smaller radii of curvature (<2 in.) tended to create a toroidal potential well in which a droplet "orbits." The 3-in. radius reflector ultimately used allowed stable levitation with a relatively low standing wave intensity and, hence, a low degree of static deformation in excess of what is required for levitation. However, it seems reasonable to say the shape of the potential well impacts the static shape of the droplet just as it does in electromagnetic levitation (where the droplet takes on a "pear" shape characteristic of Y_{30} due to the "basket-shaped" potential well). Since the radial focus of the potential well is a necessary evil in Earth-based levitators, one area for future work might involve study of the shape of the potential well and optimization of the acoustic reflector shape to balance the need for radial focus with the effect on the static shape of the droplet.

Acknowledgments

This project has been carried out thanks to support from NASA under Grant NAGW-2845 and the National Science Foundation under Grant CTS 9312379. The authors would also like to acknowledge the gracious technical assistance of Rod Shampine.

References

[1]Egry, I., Lohofer, G., Neuhaus, P., and Sauerland, S., "Surface Tension Measurements of Liquid Metals Using Levitation, Microgravity, and Image Processing," *International Journal of Thermophysics*, Vol. 13, No. 1, 1992, pp. 65–94.

[2]Miller, C. A., and Scriven, L. E., "The Oscillations of a Fluid Droplet Immersed in Another Liquid," *Journal of Fluid Mechanics*, Vol. 32, No. 3, 1968, pp. 417–435.

[3]Prosperetti, A., "Normal-Mode Analysis for the Oscillations of a Viscous Liquid Drop in an Immiscible Liquid," *Journal de Mecanique*, Vol. 19, No. 1, 1980, pp. 149–182.

[4]Kelvin, L., "Oscillations of a Liquid Sphere," *Mathematical and Physical Papers*, Vol. 3, Clay and Sons, London, 1890, pp. 384–386.

[5]Chandrasekhar, S., *Hydrodynamic and Hydromagnetic Stability*, Clarendon, Oxford, England, UK, 1961, pp. 467–480.

[6]Rayleigh, J. W. S., "The Equilibrium of Revolving Liquid Under Capillary Force," *Philosophical Magazine*, Vol. 28, 1914, pp. 161–170.

[7]Lamb, H., *Hydrodynamics*, 6th ed., Dover, New York, 1945, p. 473.

[8]Busse, F. H., "The Oscillations of a Rotating Liquid Drop," *Journal of Fluid Mechanics*, Vol. 142, No. 1, 1984, pp. 1–8.

[9]Bayazitoglu, Y., and Suryanarayana, P. V. R., "Dynamics of Oscillating Viscous Droplets Immersed in Viscous Media," *Acta Mechanica*, Vol. 95, 1992, pp. 167–183.

[10]Basaran, O., "Nonlinear Oscillations of Viscous Liquid Drops," *Journal of Fluid Mechanics*, Vol. 241, 1992, pp. 169–198.

[11]Daidzic, N., Stadler, R., and Schrankler, S., "Nonlinear Droplet Oscillations," *Proceedings of the 7th Workshop on Two-Phase Flow Predictions* (Erlangen, Germany), 1994.

[12]Marston, P. L., "Shape Oscillation and Static Deformation of Drops and Bubbles Driven by Modulated Radiation Stresses—Theory," *Journal of the Acoustical Society of America*, Vol. 67, No. 1, 1980, pp. 15–26.

[13]Cummings, D. L., and Blackburn, D. A., "Oscillations of Magnetically Levitated Aspherical Droplets," *Journal of Fluid Mechanics*, Vol. 224, 1991, pp. 395–413.

[14]Suryanarayana, P. V. R., and Bayazitoglu, Y., "Effect of Static Deformation and External Forces on the Oscillations of Levitated Droplets," *Physics of Fluids A*, Vol. 3, No. 5, 1991, pp. 967–977.

[15]Barmatz, M., "Overview of Containerless Processing Technologies," *Material Processing in the Reduced Gravity Environment of Space*, edited by G. E. Rindone, Elsevier, Amsterdam, 1982, pp. 25–36.

[16]Marston, P. L., and Apfel, R. E., "Quadrupole Resonance of Drops Driven by Modulated Acoustic Radiation Pressure—Experimental Properties," *Journal of the Acoustical Society of America*, Vol. 67, No. 1, 1980, pp. 27–37.

[17]Trinh, E., Zwern, A., and Wang, T. G., "An Experimental Study of Small-Amplitude Drop Oscillations in Immiscible Liquid Systems," *Journal of Fluid Mechanics*, Vol. 115, 1982, pp. 453–474.

[18]Trinh, E. H., and Hsu, C.-J., "Equilibrium Shapes of Acoustically Levitated Drops," *Journal of the Acoustical Society of America*, Vol. 79, No. 5, 1986, pp. 1335–1338.

[19]Tian, Y., Holt, R. G., and Apfel, R. E., "Deformation and Location of an Acoustically Levitated Liquid Drop," *Journal of the Acoustical Society of America*, Vol. 93, No. 6, 1993, pp. 3096–3104.

[20]Trinh, E. H., and Hsu, C.-J., "Acoustic Levitation Methods for Density Measurements," *Journal of the Acoustical Society of America*, Vol. 80, No. 6, 1986, pp. 1757–1761.

[21]Trinh, E., Marston, P. L., and Robey, J. L., "Acoustic Measurement of the Surface Tension of Levitated Drops," *Journal of Colloid and Interface Science*, Vol. 124, No. 1, 1988, pp. 95–103.

[22]Daidzic, N., Stadler, R., and Dominick, J., "Experimental Techniques for Measurement of Droplet Evaporation," *ICLASS-94: Proceedings of the Eighth International Conference on Liquid Atomization and Spray Systems*, National Inst. of Standards and Technology, Rouen, France, 1994, pp. 875–882.

[23]Krishnan, S., Hansen, G. P., Hauge, R. H., and Margrave, J. L., "Observations on the Dynamics of Electromagnetically Levitated Liquid Metals and Alloys at Elevated Temperatures," *Metallurgical Transactions A*, Vol. 19A, Aug. 1988, pp. 1939–1943.

[24]Mitchell, G. F., "The Measurement of Surface Tension and Viscosity via Acoustic Levitation," M.S. Thesis, Rice Univ., Houston, TX, April 1995.